Research Article

Lijun Zhou*, Yingyi Xia, Woyang Li, Qian Lei, Yunyun Qian, Xiaohu Cai, Lei Guo, and Dongyang Wang

Molecular dynamics simulation of thermodynamic properties of Al_2O_3-modified silicone rubber under silane coupling agent modification

https://doi.org/10.1515/epoly-2024-0055
received May 27, 2024; accepted June 24, 2024

Abstract: Silicone rubber is renowned for its excellent insulating properties. Enhancing its thermal conductivity can significantly improve its performance, making it more suitable for the demanding conditions of operational transformers. Adding liquid silicone rubber (ALSR) with high-performance fillers modified by coupling agents effectively enhances its thermal conductivity. This study used molecular dynamics simulations to construct Al_2O_3/ALSR models with unmodified and 3-aminopropyltriethoxysilane (KH550) silane coupling agent-modified alumina at grafting rates of 5% and 10%. The effects of different grafting rates of surface-modified Al_2O_3 on the thermodynamic properties and microstructure of silicone rubber composites were analyzed. The study found that the modification with the KH550 silane coupling agent significantly enhanced the thermodynamic properties of Al_2O_3/ALSR composites. Compared to the model without a grafting coupling agent, the thermal conductivity of the composite materials with grafting rates of 5% and 10%, respectively, increased by 97.91% and 127.75%. Simultaneously, excessive content of silane coupling agents can lead to instability in the molecular interface structure, resulting in a decline in the composite materials' thermal stability and mechanical properties. By examining the free volume and mean square displacement of the composite materials, it is observed that the surface modification of Al_2O_3 with the silane coupling agent KH-550 restricts the mobility of silicone rubber molecular chains. However, as the grafting rate increases, this hindering effect diminishes, consequently reducing the interfacial adhesion of Al_2O_3/ALSR.

Keywords: ALSR, silane coupling agent, Al_2O_3, molecular dynamics simulation, thermodynamic property

1 Introduction

Dry-type distribution transformers constitute pivotal assets within power distribution networks, boasting a substantial installed base (1–3). Nevertheless, the magnitude of units rendered obsolete annually is considerable. Effectively handling decommissioned dry-type distribution transformers to achieve their green recyclability is crucial for power grids to attain their "dual-carbon" goals (4,5). Traditional dry-type transformers employ epoxy resin as the principal insulation material, which is prone to moisture absorption and lacks recyclability or reusability upon decommissioning. This characteristic poses a significant risk of energy and resource wastage (6–10). Utilizing recyclable elastomeric materials for insulation in dry-type transformers significantly reduces carbon emissions and enhances the safety of grid operations and the economic viability of transformer units by effectively mitigating frequent expansion and contraction stresses.

Silicone rubber possesses characteristics such as high elasticity, resistance to extreme temperatures, excellent hydrophobicity, superior insulation properties, and safety, making it a viable alternative material (11–13). However, their intrinsic thermal conductivity is approximately around 0.17 $W \cdot m^{-1} \cdot K^{-1}$ for silicone rubber matrices, which is relatively low. This low thermal conductivity limits their application in dry-type transformers (14,15). As real-world operating conditions become increasingly complex and demanding, there is a growing demand for improved thermal conductivity and heat resistance of silicone rubber. Therefore, the thermodynamic properties of silicone rubber materials can

* **Corresponding author: Lijun Zhou**, School of Electrical Engineering, Southwest Jiaotong University, Chengdu, 611756, China,
e-mail: ljzhou10@163.com
Yingyi Xia, **Woyang Li**, **Qian Lei**, **Yunyun Qian**, **Xiaohu Cai**, **Lei Guo**, **Dongyang Wang:** School of Electrical Engineering, Southwest Jiaotong University, Chengdu, 611756, China

be enhanced by incorporating high-performance fillers into the silicone rubber matrix (16,17).

The choice of fillers significantly impacts the thermal conductivity of filled polymers. Currently, various types of fillers are employed to enhance thermal conductivity, including metallic fillers (such as copper, silver, and aluminum), carbon-based fillers (like graphite, carbon nanotubes, and graphene), and inorganic fillers (such as aluminum oxide, aluminum nitride, and boron nitride) (18–21). Sun et al. found that by incorporating 30 wt% h-BN into epoxy resin, the thermal conductivity of h-BN/EP composite materials can reach 0.86 $W \cdot m^{-1} \cdot K^{-1}$ (22). Li et al. conducted a study and found that under a fixed filler loading of 120 phr, spherical aluminum oxide, irregular aluminum nitride, and two-dimensional boron nitride flakes exhibit varying effects on the thermal conductivity of liquid silicone rubber, with respective increases in thermal conductivity coefficients of 88%, 124%, and 316% (23). Although BN exhibits a higher enhancement effect on the thermal conductivity of silicone rubber compared to Al_2O_3, the mechanical performance improvement of Al_2O_3 far exceeds that of BN and is also more cost-effective. Therefore, aluminum oxide is widely used in industrial applications (24). However, Al_2O_3 tends to aggregate, making it difficult to disperse evenly within the silicone rubber matrix when directly incorporated. This aggregation can lead to poor interfacial bonding and defects at the molecular interface, thereby hindering the enhancement of adding liquid silicone rubber (ALSR) performance (25). Preventing filler aggregation and ensuring uniform dispersion within the matrix material is crucial for enhancing composite material performance. Chemical modification or functionalization of filler surfaces can effectively avoid aggregation phenomena (26,27). Kim et al. employed the silane coupling agent KH550 for surface modification of aluminum powder. Experimental results demonstrated that the surface-modified fillers significantly enhanced the composite materials' fracture toughness, wear resistance, and adhesive strength (28).

To enhance the adhesion at the Al_2O_3/ALSR molecular interface and facilitate better dispersion of Al_2O_3 within the ALSR matrix, this study constructed models of unmodified Al_2O_3/ALSR as well as Al_2O_3/ALSR modified with KH550 silane coupling agent at grafting rates of 5% and 10%. The analysis and comparison of the effects of different grafting rates of surface-modified Al_2O_3 on the thermodynamic properties and microstructure of silicone rubber composite materials were conducted. Furthermore, the study investigated the influence of coupling agent content on the performance of silicone rubber composite materials, aiming to lay the groundwork for the subsequent development of new-generation environmentally friendly, dry-type recyclable transformers insulation materials.

2 Model establishment

2.1 Initial model construction

Using Material Studio software, monomer models of ALSR and Al_2O_3 molecules were separately constructed. VPDMS was selected as the base polymer, with PMHS as the crosslinking agent. Each VPDMS single chain consisted of 20 repeating units, while each PMHS single chain comprised 15 repeating units. Surface modification of Al_2O_3 molecules was performed using KH550 with grafting rates of 5% and 10%. Given the high molecular weight and initial polymerization degree of ALSR, simulating a large number of repeating unit molecules is impractical. This study examines the influence of different grafting rates of silane coupling agent-modified Al_2O_3 molecules on ALSR performance. Considering computational efficiency and ensuring sufficient crosslinking, 12 VPDMS chains and 6 PMHS chains were used to construct the pure silicone rubber model.

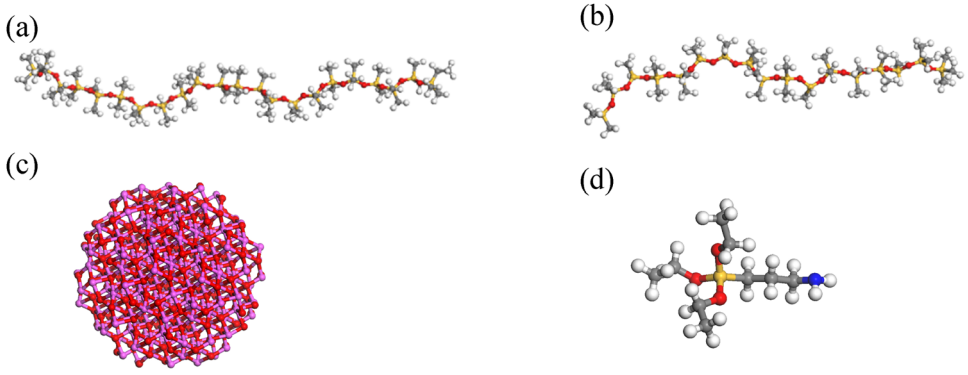

Figure 1: The individual monomer models: (a) VPDMS, (b) PMHS, (c) Al_2O_3, (d) KH550.

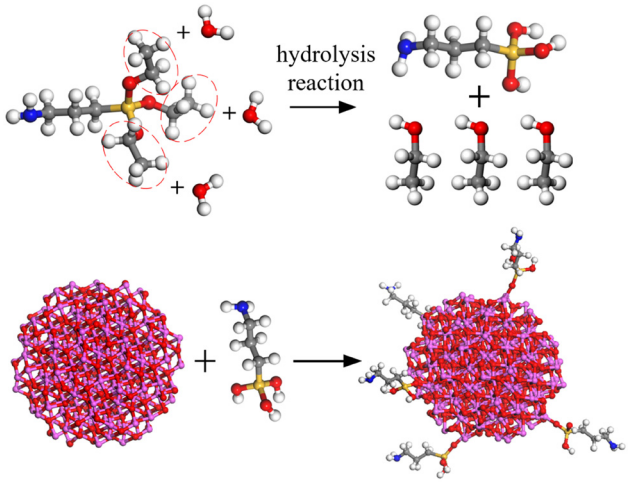

Figure 2: Silane coupling agent modification process.

The monomer models are depicted in Figure 1, while the KH550 silane coupling agent modification process is illustrated in Figure 2.

2.2 Model construction steps

1. The models of pure silicone rubber, silicone rubber doped with Al_2O_3, and Al_2O_3/ALSR with different grafting rates were constructed separately. The models of pure silicone rubber and silicone rubber doped with Al_2O_3 and Al_2O_3/ALSR with different grafting rates were independently built. The initial models were established using the amorphous cell module, with an initial density of 0.6 $g \cdot cm^{-3}$ and a doping ratio of 30% for Al_2O_3. The model of pure silicone rubber is denoted as ALSR, silicone rubber doped with Al_2O_3 is ALSR-1, silicone rubber doped with 5% KH-550 grafted Al_2O_3 is ALSR-2, and silicone rubber doped with 10% KH-550 grafted Al_2O_3 is ALSR-3.
2. First, the initial model of pure silicone rubber undergoes geometric optimization (10,000 steps) to minimize the model energy. After geometric optimization, the model undergoes a 200 ps dynamic optimization under the NVT ensemble at a temperature of 600 K. Subsequently, a 100 ps dynamic optimization under the NPT ensemble is conducted at the same temperature. Since the remaining three models all contain Al_2O_3, to prevent deformation during the optimization process, it is necessary to fix the structures of Al_2O_3 and its grafted molecules before the optimization. Following this, geometric optimization and a 200 ps dynamic optimization under the NVT ensemble at 600 K are conducted separately for each model. The final optimized models obtained are depicted in Figure 3, which will be used for subsequent cross-linking.
3. The cross-linking reaction proceeds as follows: under the catalysis of a catalyst, ethylene reacts with polyhydrosiloxane through a hydrosilylation addition reaction, forming new Si–C bonds, which leads to the cross-linking of polysiloxane into a network structure. Typically,

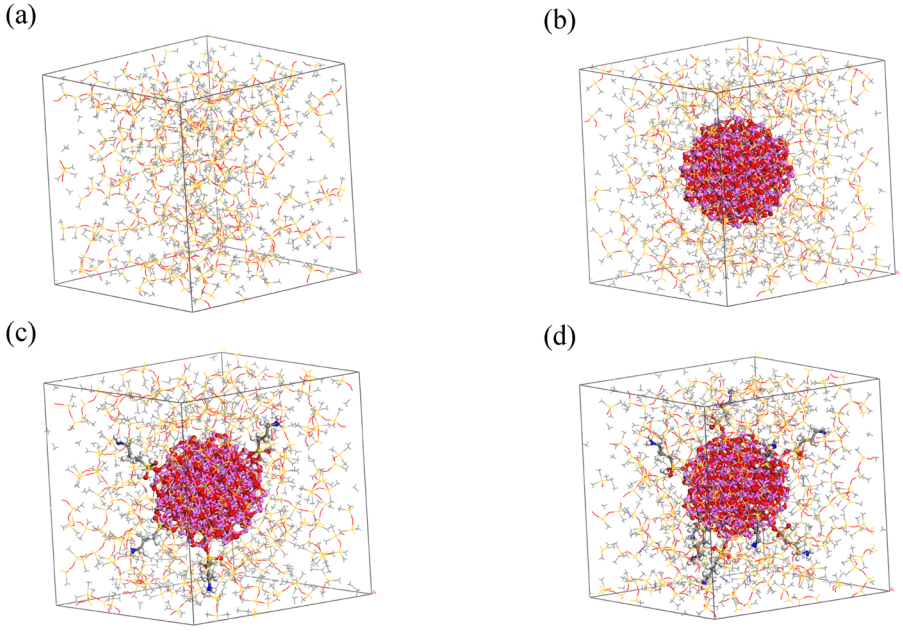

Figure 3: Optimized models before cross-linking: (a) ALSR, (b) ALSR-1, (c) ALSR-2, and (d) ALSR-3.

platinum-based catalysts are chosen for this purpose. The cross-linking reaction equation is shown in Figure 4. The simulation of the cross-linking reaction can be achieved through a Perl script. The initial reaction radius is 3.5 Å, the maximum reaction radius is 8 Å, and the step size is 0.5 Å. The cross-linking temperature is 438 K, and the maximum cross-linking degree is 90%.

2.3 Cross-linking model optimization

The cross-linked models obtained cannot be further investigated for performance parameters due to excessive internal stress in the system. Therefore, structural optimization and dynamic optimization are required for these models. First, geometric optimization is performed on the models, followed by five cycles of annealing under the NVT ensemble within the temperature range of 300–600 K, with a total simulation time of 140 ps. After annealing cycles, the model with the lowest potential energy is selected for a 100 ps NPT dynamic simulation at 600 K. Subsequently, dynamic simulations are conducted at 300 K, starting with a 200 ps NVT simulation followed by a 100 ps NPT simulation. The resulting model is then used for subsequent molecular simulation calculations. The final optimized cross-linked model is depicted in Figure 5, while the cross-linking bonds are illustrated in Figure 6.

In the simulation process, temperature and pressure were controlled using the Andersen and Berendsen methods. The pure silicone rubber model employed the COMPASSII force field, while the remaining models utilized the Universal force field. Electrostatic and van der Waals forces were calculated using the Ewald and Atom-based methods.

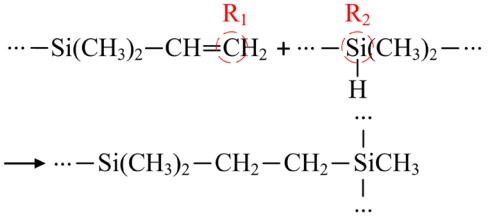

Figure 4: Cross-linking reaction.

3 Thermodynamic performance calculation

3.1 Thermal conductivity

Various methods based on molecular dynamics have been extensively researched for calculating material thermal conductivity, such as Green-Kubo, non-equilibrium molecular dynamics, and reverse non-equilibrium molecular dynamics (RNEMD). RNEMD is widely adopted among these due to its high accuracy and fast convergence rate.

This article utilizes the RNEMD method to compute thermal conductivity. The model is evenly divided along

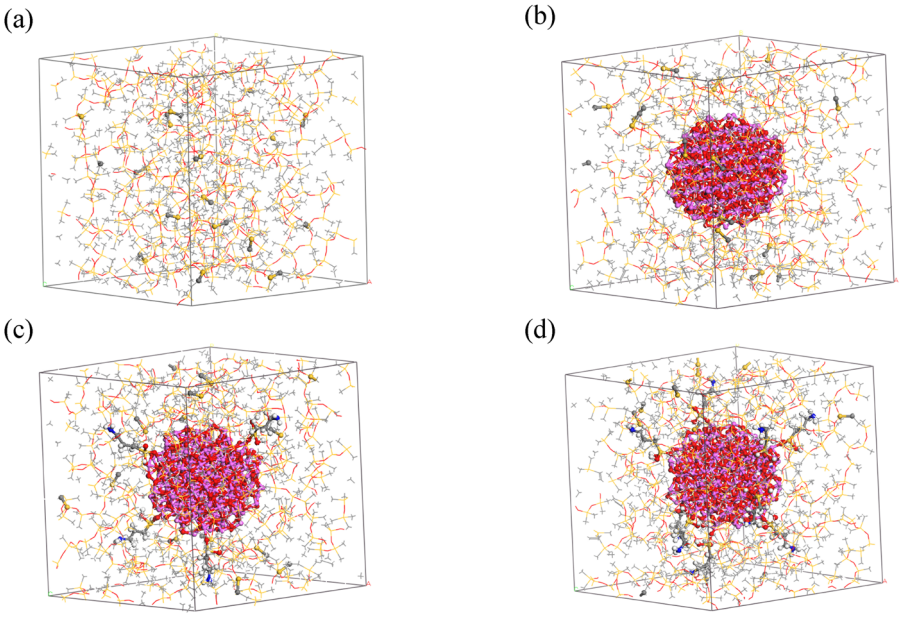

Figure 5: Optimized models after cross-linking: (a) ALSR, (b) ALSR-1, (c) ALSR-2, and (d) ALSR-3.

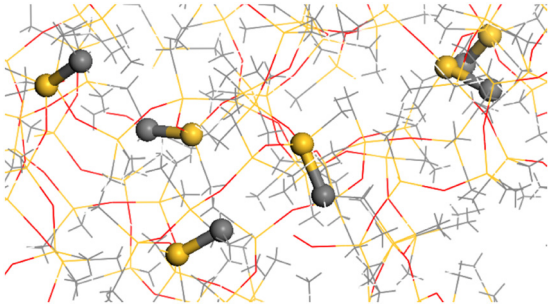

Figure 6: Cross-linking bonds.

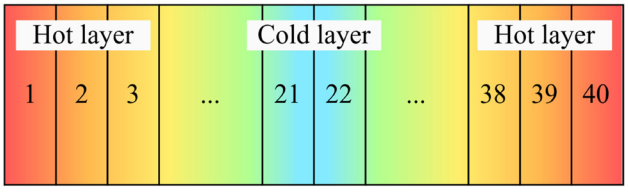

Figure 7: Schematic diagram of the RNEMD method model.

a specific direction (in this study, the *z*-direction) into several layers (a total of 40 layers in this paper), with the outermost layers at both ends of the model termed the "hot layers" and the middle two layers referred to as the "cold layers," as illustrated in Figure 7.

Then, energy exchange occurs by exchanging kinetic energy between the coldest particles in the hot layers and the hottest particles in the cold layers. After multiple energy exchanges and averaging, a stable temperature gradient is established within the system. The thermal conductivity λ is calculated based on Fourier's heat conduction law.

$$\lambda = -\frac{J}{\mathrm{d}T/\mathrm{d}z} \tag{1}$$

where J represents the energy flux in the *z*-direction and $\mathrm{d}T/\mathrm{d}z$ represents the temperature gradient. The negative sign indicates that the direction of energy flux is always opposite to the temperature gradient.

The energy flux J can be represented by the energy exchange ΔE between two fixed layers during each time interval Δt.

$$J = \frac{1}{2A} \times \frac{\Delta E}{\Delta t} \tag{2}$$

where A represents the area perpendicular to the model's energy flux direction.

When calculating the thermal conductivity of materials, it is necessary to reconstruct the thermal conductivity calculation model while keeping the number and types of molecular chains within the unit cell unchanged. The model is enlarged by a factor of three along the *z*-direction to facilitate the formation of a stable temperature gradient within the system, thus enabling the calculation of thermal conductivity more effectively. When a stable temperature gradient is established within the system, the temperature variation along the *z*-direction of the model is depicted in Figure 8. The calculated thermal conductivity values for different types of silicone rubber are illustrated in Figure 9.

The results reveal that after doping with 30% Al_2O_3, the thermal conductivity of silicone rubber increased from 0.177 to 0.191 $W \cdot m^{-1} \cdot K^{-1}$, with the improvement not being

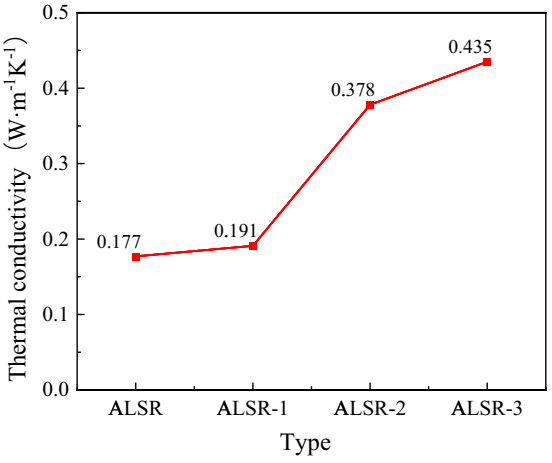

Figure 9: Thermal conductivity of different types of silicone rubber.

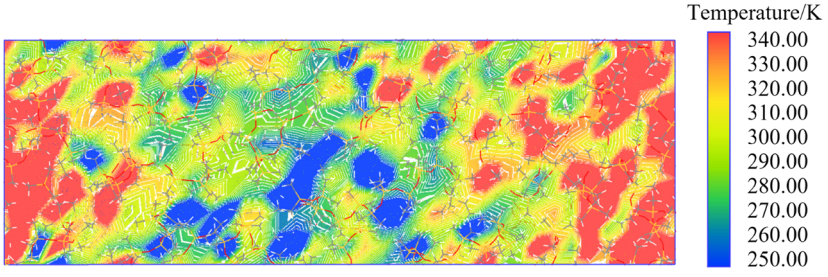

Figure 8: Temperature distribution of the calculated model.

significant. However, the thermal conductivity is greatly enhanced after modifying alumina with a KH-550 silane coupling agent. When the grafting rate of KH-550 is 5%, the thermal conductivity reaches 0.378; when the grafting rate is 10%, the thermal conductivity increases to 0.435. The thermal conductivity of the Al_2O_3 surface modified with silane coupling agent exhibits a significant increase compared to its unmodified state. The main reason is the addition of the coupling agent, which enhances the connection between Al_2O_3 molecules and silicone rubber chains, resulting in a tighter bond between them and a more pronounced modification effect. Similarly, the higher the grafting rate of the coupling agent, the more significant the enhancement effect on thermal conductivity.

3.2 Glass transition temperature

The glass transition temperature (T_g) is the critical temperature at which amorphous materials (such as glass) transition from liquid to solid as the temperature decreases. This temperature marks a significant transition in the material's structure and properties, shifting from a disordered liquid state to an ordered solid state. At the microscopic level, T_g represents the temperature at which polymer chain segment motion can be activated, making it one of the critical characteristic indicators of polymer properties.

The relationship between material density and temperature can be obtained through molecular dynamics simulations of cooling experiments. The cooling range is set from 100 to 350 K with a cooling rate of 10 K per 250 ps, and molecular dynamics simulations are conducted under the NVT and NPT ensembles for 100 ps at each temperature, resulting in 25 sets of density–temperature data. By analyzing the density–temperature curve, the material's T_g can be determined. Specifically, when a distinct inflection point appears on the curve, linear regression is applied to the data on both sides of the inflection point to obtain the intersection point T_g of the two linear fits, as illustrated in Figure 10.

The graph shows that when no coupling agent is used, there is no significant change in the T_g of Al_2O_3/ALSR compared

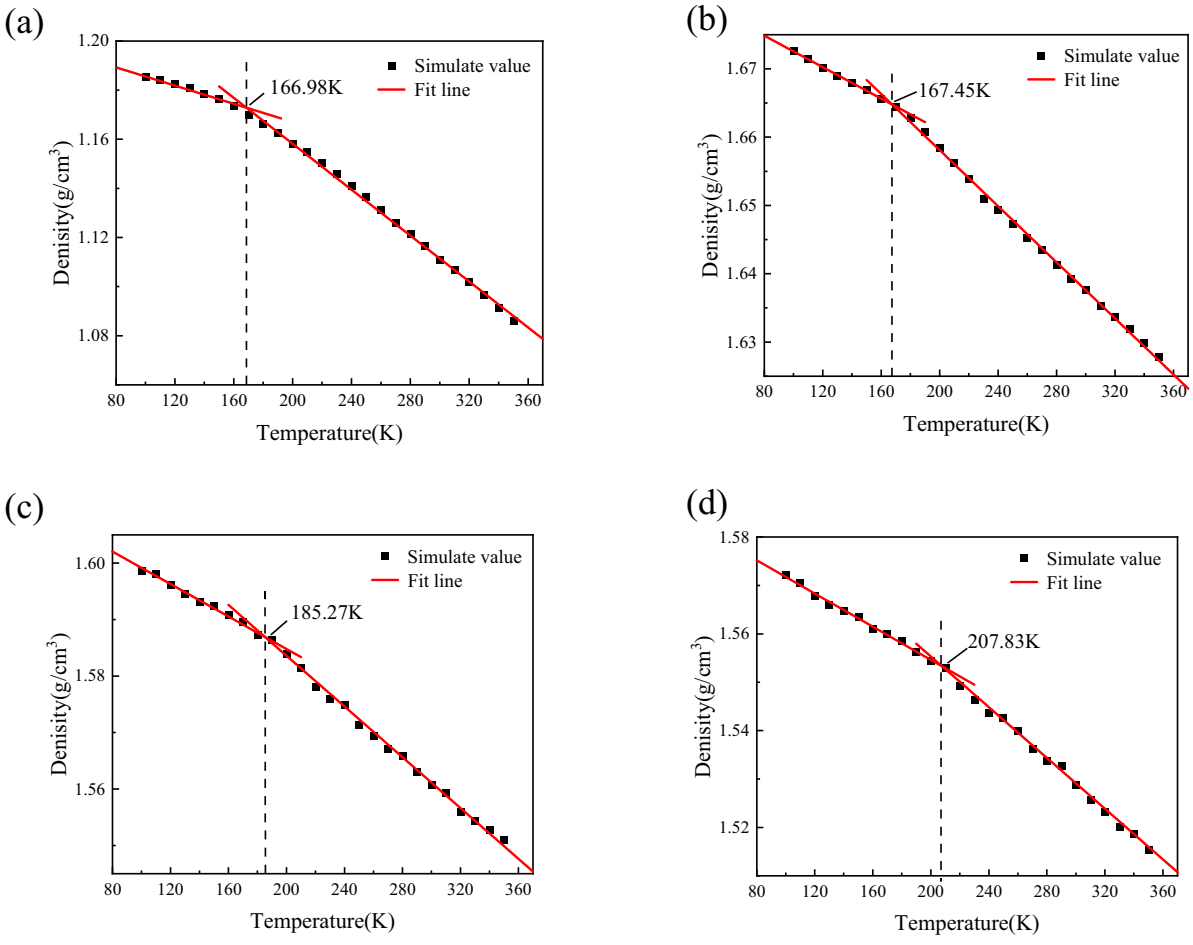

Figure 10: Schematic of linear fitting of density-temperature curves: (a) ALSR, (b) ALSR-1, (c) ALSR-2, (d) ALSR-3.

to pure silicone rubber. However, the model's T_g is significantly increased after using the coupling agent. Specifically, with a grafting rate of 5%, T_g is 185.27 K, and with a grafting rate of 10%, T_g is 207.83 K. Compared to the model with Al_2O_3 doping but without coupling agent grafting, there is an increase of 10.65% and 24.11%, respectively. This indicates that the surface modification of Al_2O_3 with KH-550 silane coupling agent impedes the motion of silicone rubber molecular chains, thus requiring higher temperatures to activate the motion of silicone rubber chain segments. For both models before and after coupling agent grafting, the sharp increase in T_g is mainly attributed to adding the coupling agent, which improves the aggregation phenomenon of alumina. This improves bonding between Al_2O_3 and the silicone rubber matrix, enhancing the molecular interface adhesion between Al_2O_3 and silicone rubber. It effectively assists in the modification of Al_2O_3-reinforced silicone rubber, improving the overall performance of silicone rubber.

3.3 Coefficient of thermal expansion (CTE)

The CTE represents the percentage change in the volume of a unit of material when the temperature changes. Understanding the CTE of a material allows for predicting dimensional changes of an object when subjected to temperature variations, thereby avoiding structural deformation, cracks, or damage caused by thermal expansion. It is an important indicator for measuring the thermal stability of materials.

The volume and temperature of the system before and after the glass transition temperature are fitted to obtain the corresponding temperature–volume curves, as shown in Figure 11. From Figure 11, the slope of the fitting curve before and after the material's T_g can be obtained. Then, the thermal expansion coefficients of the glassy state (below T_g) and the rubbery state (above T_g) of each system are calculated using Eq. 3, and the results are presented in Table 1.

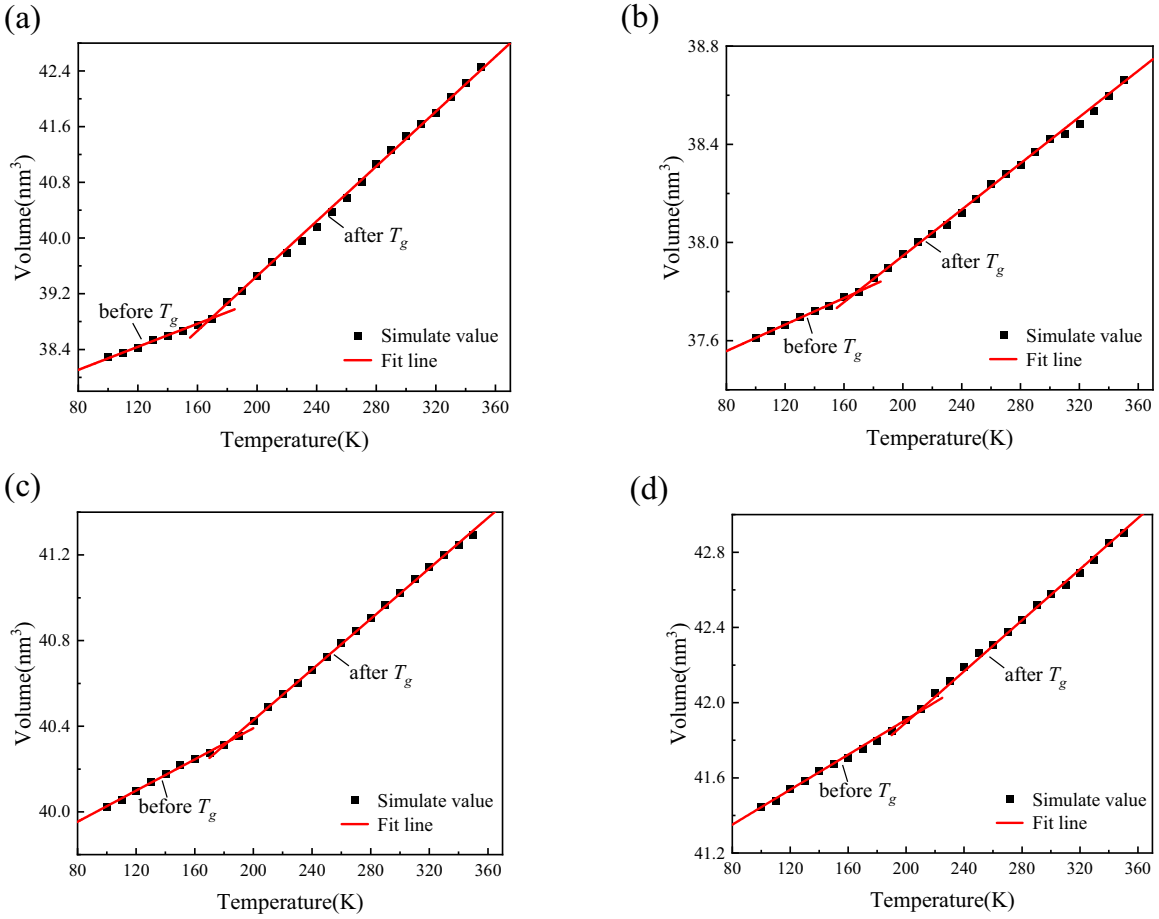

Figure 11: Schematic of linear fitting of volume–temperature curves: (a) ALSR, (b) ALSR-1, (c) ALSR-2, and (d) ALSR-3.

Table 1: CTE for different types of silicone rubber

Type	Glassy state β_{CTE} (K^{-1})	Rubbery state β_{CTE} (K^{-1})
ALSR	1.94×10^{-4}	4.66×10^{-4}
ALSR-1	0.71×10^{-4}	1.23×10^{-4}
ALSR-2	0.89×10^{-4}	1.44×10^{-4}
ALSR-3	1.09×10^{-4}	1.59×10^{-4}

$$\beta_{\mathrm{CTE}} = \frac{1}{V_0}\left(\frac{\partial V}{\partial T}\right)_P \tag{3}$$

where β_{CTE} represents the CTE, V_0 denotes the volume of the model at the initial temperature, and P is 0.0001 GPa.

Table 1 shows that Al_2O_3 can alter silicone rubber's thermal expansion coefficient, resulting in a significant reduction in CTE for both its glassy and rubbery states. However, after grafting with the silane coupling agent KH-550, the CTE of the thermal expansion system compared to the nongrafting model exhibits a slight increase, which further increases with an increase in the grafting rate. Compared to pure silicone rubber, the postgrafting model exhibits considerably lower coefficients of thermal expansion, indicating that the incorporation of Al_2O_3 enhances the thermal stability of silicone rubber. The increase in the CTE after grafting with the coupling agent is likely due to the poor thermal stability of the coupling agent itself, which leads to changes in the thermal expansion coefficient of the composite material.

3.4 Mechanical properties

Molecular dynamics simulations can be employed to analyze stress and strain in systems undergoing minor deformation, enabling the extraction of parameters relevant to mechanical properties. Due to the isotropic behavior exhibited by silicone rubber on a macroscopic scale, it can be approximately treated as an isotropic material. Its bulk modulus K, Young's modulus E, and shear modulus G can be obtained from the following formulas:

$$K = \lambda + \frac{2}{3}\mu \tag{4}$$

$$E = \mu\frac{3\lambda + 2\mu}{\lambda + \mu} \tag{5}$$

$$G = \mu \tag{6}$$

where λ and μ are constants that can be obtained through molecular dynamics calculations.

For models of silicone rubber and its modified materials, a geometric optimization is performed at 300 K to minimize the stress within the system as much as possible. The geometrically optimized models are then subjected to 100 ps of NPT dynamic calculations, with a model output generated every one ps, resulting in a total of 100 models. The five models with the lowest potential energy are selected, and mechanical performance calculations are conducted using the constant strain method, with a maximum strain set to 0.003. Finally, the values of λ and μ for each model at 300 K are obtained, and according to Eqs. 4–6, the corresponding models' bulk modulus K, Young's modulus E, and shear modulus G are calculated, resulting in five sets for each parameter. The average values are then taken to obtain the final results, as shown in Table 2. Figure 12 displays the mechanical properties of each system.

From the graph, it can be observed that the addition of Al_2O_3 increases the bulk modulus, Young's modulus, and shear modulus of silicone rubber. This indicates that doping with Al_2O_3 enhances the rigidity of silicone rubber, making it less prone to deformation. After modification with the KH-550 silane coupling agent, the bulk modulus, Young's modulus, and shear modulus of silicone rubber are significantly enhanced. Specifically, when the grafting rate is 5%, the silicone rubber shows a much more significant increase in these properties than pure silicone rubber and silicone rubber without the coupling agent. The bulk modulus increases by 881.8% and 329.4%, Young's modulus increases by 451.4% and 175.4%, and the shear modulus increases by 372.5% and 101.3%, respectively. This indicates that after grafting with the silane coupling agent, the adhesion between Al_2O_3 and the silicone rubber matrix surface increases, making the silicone rubber composite system more stable and less prone to deformation under external forces. However, with the rise in grafting rate to 10%, a decline in mechanical performance relative to the 5% grafting rate is observed. This phenomenon may stem from the heightened concentration of the silane coupling agent at higher grafting rates, leading to potential instability in the molecular interface structure. Such instability could manifest as excessive aggregation or crystallization within the molecular interface layer, resulting in deformation and subsequent reduction in adhesion. Consequently,

Table 2: Mechanical properties of different types of silicone rubber models

Type	*K*	*E*	*G*
ALSR	1.92	5.02	2.36
ALSR-1	4.39	10.05	5.54
ALSR-2	18.85	27.68	11.15
ALSR-3	16.42	18.86	7.41

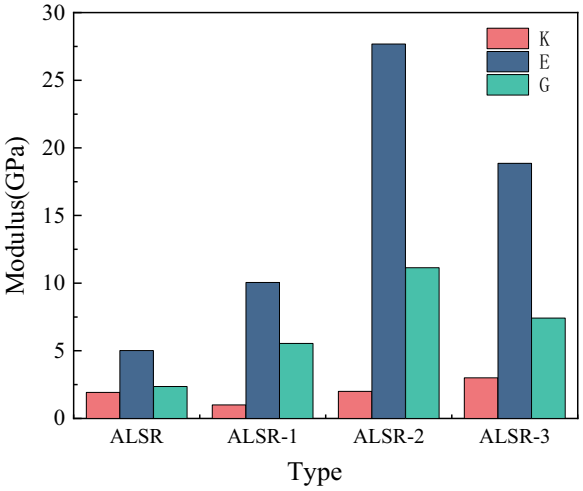

Figure 12: Mechanical properties of different types of silicone rubber models.

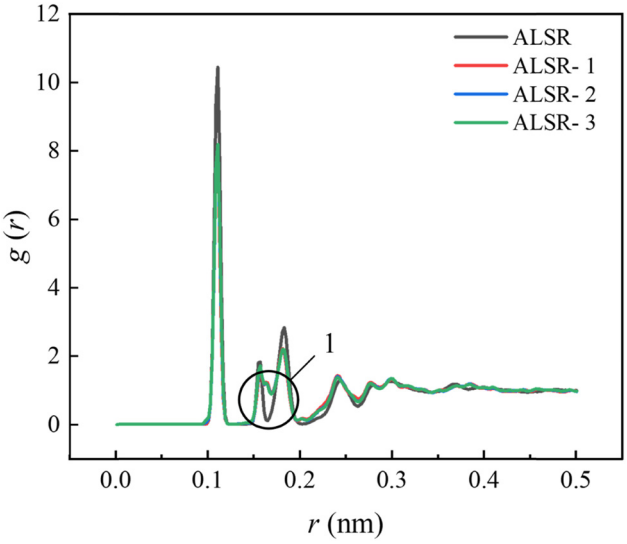

Figure 13: Full atomic RDF for the four system models.

this adverse effect on adhesion could impact the mechanical properties, decreasing overall mechanical performance.

4 Structural parameter calculation

4.1 Radial distribution function (RDF)

The RDF is a parameter reflecting the microstructural characteristics of materials, capable of revealing the nature of interactions between nonbonded atoms. It is defined as follows:

$$g_{\mathrm{A-B}}(r) = \frac{n_{\mathrm{B}}V}{4\pi r^2 \mathrm{d}r N_{\mathrm{B}}} \tag{7}$$

where n_{B} is the number of B atoms at a distance r around the A atom, N_{B} is the total number of B atoms, and V is the volume of the entire system.

Figure 13 shows the whole atomic RDF for all model systems. The RDF of the Al_2O_3/ALSR model exhibits an additional peak compared to the pure silicone rubber model, mainly due to the introduction of Al_2O_3. In the silicone rubber model doped with Al_2O_3, there is no significant difference in the overall trend of the whole atomic RDF before and after coupling agent modification. Differences are only observed at various peak positions.

The first peak of the RDF for all four types of silicone rubber occurs at 0.111 nm. The peak of pure silicone rubber is the highest, indicating the presence of a large number of C–H covalent bonds in all silicone rubber models. However, in the Al_2O_3/ALSR model, other covalent bonds in the system affect the proportion of C–H covalent bonds. In addition, the Al_2O_3/ALSR model exhibits a third peak not present in the pure silicone rubber model, as indicated by circle 1 in Figure 13. This peak corresponds to the Al–O covalent bonds in the system, effectively demonstrating the doping of Al_2O_3 in the model.

4.2 Free volume

A unit cell is not entirely filled with polymer molecules in molecular simulations. The space occupied by polymer chains is called the occupied volume, while the space available for polymer chain movement is termed the free volume. The magnitude of polymer-free volume indicates intermolecular cohesion in materials; a smaller free volume suggests a denser molecular packing. Temperature also affects the free volume, thereby influencing the performance of polymer materials, such as the glass transition temperature. The formula for calculating the fractional free volume (FFV) is as follows:

$$\mathrm{FFV} = \frac{V_{\mathrm{f}}}{V_0 + V_{\mathrm{f}}} \tag{8}$$

where V_{f} represents the free volume and V_0 represents the occupied volume.

Figure 14 displays the free volume (depicted in blue) of the pure silicone rubber model and the Al_2O_3/ALSR model at a temperature of 300 K. Table 3 presents the occupied volume, free volume, and the FFV calculated using Eq. 8 for the simulated silicone rubber model.

The results indicate that the FFV of the pure silicone rubber model is the highest, at 13.20%, while the FFV of the Al_2O_3/ALSR model decreases to 9.27%. Furthermore, the FFV decreases again after grafting with the silane coupling

agent and decreases further with increasing grafting rate. This indicates that the surface modification of Al_2O_3 by the silane coupling agent KH-550 hinders the movement of silicone rubber molecular chains, with the hindrance effect becoming more pronounced as the grafting rate increases.

Table 3: FFV of different types of silicone rubber

Type	V_f (nm^3)	V_o (nm^3)	FFV (%)
ALSR	5.315	34.951	13.20
ALSR-1	2.785	36.656	9.27
ALSR-2	3.956	38.721	7.21
ALSR-3	3.081	39.624	7.06

4.3 Mean square displacement (MSD)

The atoms within the system exhibit continuous motion, and the indicator used to describe the mobility of polymer chains is called MSD, which specifically refers to the average of the squared displacements of particles in the system, defined as follows:

$$\mathrm{MSD} = \frac{1}{3N}\sum_{i=0}^{N-1}(|R_i(t) - R_i(0)|^2) \tag{9}$$

where $R_i(t)$ and $R_i(0)$ represent the displacement vectors of any atom i within the system at time t and the initial time, respectively.

At 300 K, the models underwent MSD analysis, resulting in MSD curves for the pure silicone rubber system and the Al_2O_3/ALSR system, as depicted in Figure 15. The graph shows that the MSD values of the silicone rubber composite materials doped with Al_2O_3 and grafted with coupling agents both exhibit a decreasing trend. However, when the coupling agent content increases from 5% to 10%, a slight upward trend in MSD is observed. This indicates that adding Al_2O_3 effectively impedes the movement of silicone rubber molecular chains, and the modification by coupling agents further enhances this inhibitory effect, rendering the system more stable. At the same time, the increase in MSD with the increase in coupling agent content may be attributed to the higher grafting rate of the silane coupling agent, leading to an unstable molecular interface due to excessive coupling agent content.

4.4 Binding energy

The interface interaction in Al_2O_3/ALSR composite materials refers to the interaction between Al_2O_3 and silicone

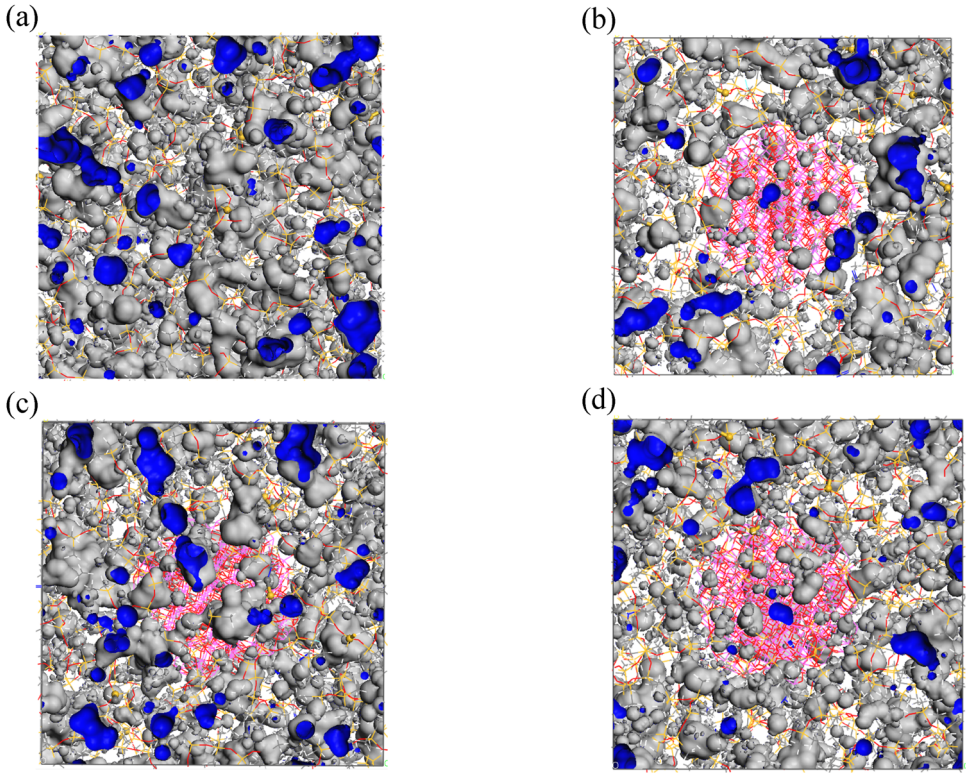

Figure 14: The distribution of free volume in different types of silicone rubber models: (a) ALSR, (b) ALSR-1, (c) ALSR-2, and (d) ALSR-3.

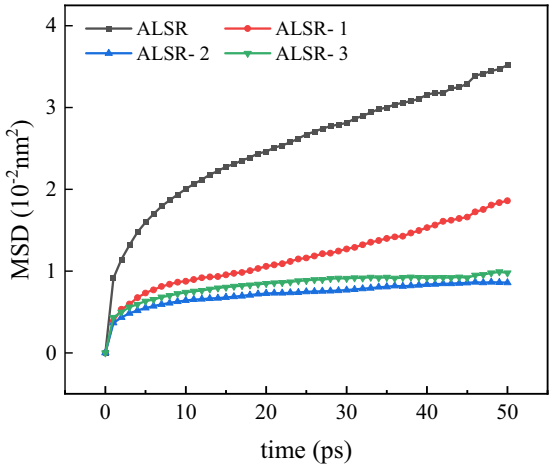

Figure 15: MSD curves in 50 ps for different systems.

rubber. The magnitude of the interface interaction significantly affects the mechanical properties of silicone rubber composite materials. Therefore, the strength of the interface interaction is commonly characterized by the intermolecular interaction energy. The calculation formula for the interaction energy ΔE of silicone rubber composite materials is as follows:

$$\Delta E = E_{\text{total}} - (E_{Al_2O_3} + E_{\text{ALSR}}) \tag{10}$$

where E_{total} represents the total potential energy of the Al_2O_3/ALSR composite material model; $E_{Al_2O_3}$ represents the total potential energy of Al_2O_3 after removing ALSR from the Al_2O_3/ALSR composite material model; and E_{ALSR} represents the total potential energy of ALSR after removing Al_2O_3 from the Al_2O_3/ALSR composite material model.

The binding energy E_{bind} is defined as the negative of the interaction energy ΔE, $E_{\text{bind}} = -\Delta E$. The calculated binding energies for different types of silicone rubber are presented in Table 4.

Table 4 shows the binding energies of the Al_2O_3/ALSR interface in the unmodified model and the model modified with silane coupling agents. The binding energy for the unmodified Al_2O_3/ALSR model is 4,616.56 kcal·mol^{-1}, while for the model with a grafting rate of 5%, the binding energy is 4,791.72 kcal·mol^{-1}, and for the model with a grafting rate of 10%, the binding energy is 5,007.46 kcal·mol^{-1}. With an increase in the grafting ratio of the coupling agent, the binding energy of the Al_2O_3/ALSR composites gradually rises. This indicates that the surface modification of Al_2O_3 by KH550 enhances the interfacial interaction between Al_2O_3 and the silicone rubber matrix, leading to a stronger bond between the ALSR matrix and the Al_2O_3 filler. Consequently, the effectiveness of the filler within the matrix is further improved.

Table 4: Binding energy of different types of silicone rubber

Type	E_{total} (kcal·mol^{-1})	$E_{Al_2O_3}$ (kcal·mol^{-1})	E_{ALSR} (kcal·mol^{-1})	E_{bind} (kcal·mol^{-1})
ALSR-1	−149,656.51	−95,433.23	−49,606.72	4,616.56
ALSR-2	−137,791.73	−82,556.97	−50,443.04	4,791.72
ALSR-3	−130,224.33	−74,857.43	−50,359.44	5,007.46

5 Conclusions

To enhance the thermal conductivity of silicone rubber insulation materials and facilitate the dispersion of Al_2O_3 within the silicone rubber matrix while concurrently improving the bonding at the Al_2O_3/ALSR molecular interface, KH550 silane coupling agents with grafting rates of 5% and 10% were selected for surface modification of Al_2O_3. Based on the analysis of molecular dynamics principles, the following conclusions were drawn:

1. Incorporating Al_2O_3 into the silicone rubber matrix can alter its thermodynamic properties. Compared to pure silicone rubber, silicone rubber composite materials doped with Al_2O_3 exhibit improvements in thermal conductivity, glass transition temperature, CTE, and mechanical properties.
2. Surface modification of Al_2O_3-doped silicone rubber with KH550 silane coupling agent effectively enhances the thermodynamic properties of silicone rubber composite materials. However, the degree of improvement varies with different grafting rates. At a coupling agent grafting rate of 10%, the thermal conductivity and glass transition temperature have increased compared to 5%. Compared to the model without coupling agent grafting, the thermal conductivity of composite materials with grafting rates of 5% and 10% increased by 97.91% and 127.75%, respectively. However, at this point, the high content of silicone coupling agents has led to instability in the molecular interface structure, resulting in a decrease in the composite material's thermal stability and mechanical performance.
3. Adding a silicone coupling agent also alters the microstructure of the composite material. Compared to the composite material without coupling agent modification, the composite material modified with coupling agent surface exhibits a decrease in free volume fraction, MSD, and an increase in binding energy. This indicates that the Al_2O_3 surface modified by the KH-550

silane coupling agent impedes the movement of silicone rubber molecular chains. However, as the grafting rate increases, the hindering effect decreases, leading to a decrease in the bonding at the Al_2O_3/ALSR molecular interface.

Funding information: This project was supported by National Natural Science Foundation of China (U1834203).

Author contributions: Lijun Zhou: writing – review and editing; Yingyi Xia: writing – original draft, conceptualization; formal analysis; Woyang Li: methodology, resources, data curation; Qian Lei: methodology, resources, data curation; Yunyun Qian: methodology, resources, data curation; Xiaohu Cai: methodology, resources, data curation; Lei Guo: visualization; Dongyang Wang: validation, writing – review and editing.

Conflict of interest: The authors state no conflict of interest.

Data availability statement: The data presented in this study are available on request from the corresponding author.

References

(1) Awadallah SK, Milanović JV, Jarman PN. The influence of modeling transformer age related failures on system reliability. IEEE Trans Power Syst. 2014;30(2):970–9.
(2) Cremasco A, Wu W, Blaszczyk A, Cranganu-Cretu B. Network modelling on dry-type transformer cooling systems. COMPEL Int J Comput Math Electr Electron Eng. 2018;37(3):1039–53.
(3) Wen M, Song J, Song Y, Liu Y, Li C, Wang P. Reliability assessment of insulation system for dry type transformers. IEEE Trans Dielectr Electr Insulation. 2013;20(6):1998–2008.
(4) Yang Z, Shang W, Zhang H, Garg H, Han C. Assessing the green distribution transformer manufacturing process using a cloud-based q-rung orthopair fuzzy multi-criteria framework. Appl Energy. 2022;311:118687.
(5) Ekinci F. An experimental determination of the optimum cooling model for dry-type transformers for different cooling configurations. Energy Sources Part A: Recovery Util, Environ Eff. 2020;42(17):2181–97.
(6) Pierce LW. An investigation of the temperature distribution in cast-resin transformer windings. IEEE Trans Power Deliv. 1992;7(2):920–6.
(7) Ohki Y. Development of epoxy resin composites with high thermal conductivity. IEEE Electr Insul Mag. 2010;26(1):48–9.
(8) Yuan S, Zhou L, Chen T, Wang D, Wang L. Thermally conductive h-BN/EHTPB/epoxy composites with enhanced toughness for on-board traction transformers. E-Polymers. 2022;22(1):821–33.
(9) Tian K, Yang S, Niu J, Wang H. Enhanced thermal conductivity and mechanical toughness of the epoxy resin by incorporation of mesogens without nanofillers. IEEE Access. 2021;9:31575–80.
(10) Liu X, Tian F, Zhao X, Du R, Xu S, Wang YZ. Multiple functional materials from crushing waste thermosetting resins. Mater Horiz. 2021;8(1):234–43.
(11) Koné D, Ghunem RA, Cissé L, Hadjadj Y, El-Hag A. Effect of residue formed during the AC and DC dry-band arcing on silicone rubber filled with natural silica. IEEE Trans Dielectr Electr Insul. 2019;26(5):1620–6.
(12) Nazir MT, Khalid A, Kabir I, Wang C, Baena JC, Akram S, et al. Flame retardancy and excellent electrical insulation performance of RTV silicone rubber. Polymers. 2021;13(17):2854.
(13) Hamdan MA, Pilgrim JA, Lewin PL. Thermo-mechanical analysis of solid interfaces in HVAC cable joints. IEEE Trans Dielectr Electr Insul. 2019;26(6):1779–87.
(14) Guo L, Ding S, Yuan S, Gou X, Cai F, Wang D, et al. Study on the thermal properties and insulation resistance of epoxy resin modified by hexagonal boron nitride. E-Polymers. 2021;21(1):681–90.
(15) Guo L, Xu H, Wu N, Yuan S, Zhou L, Wang D, et al. Molecular dynamics simulation of the effect of the thermal and mechanical properties of addition liquid silicone rubber modified by carbon nanotubes with different radii. E-Polymers. 2023;23(1):20228105.
(16) Zou Z, Wu W, Wang Y, Wang L. Enhancement of thermal conductivity and tensile strength of liquid silicone rubber by three-dimensional alumina network. Soft Mater. 2019;17(3):297–307.
(17) Li J, Zhao X, Ji X, Lu Y, Zhang L. Graphene/Alumina micro-nano hybrid network and thermal conductive and electrical insulating silicone rubber composites. Insul Mater. 2021;52(2):49–55.
(18) Dang Z, Xia Y, Zha J, Yuan J, Bai J. Preparation and dielectric properties of surface modified TiO2/silicone rubber nanocomposites. Mater Lett. 2011;65(23–24):3430–2.
(19) Zhou W, Yang Z, Feng Y, Lin L. Insights into the thermophysical properties and heat conduction enhancement of NaCl-Al2O3 composite phase change material by molecular dynamics simulation. Int J Heat Mass Transf. 2022;198:123422.
(20) Shi R, Wang X, Song X, Zhan B, Xu X, He J, et al. Tensile performance and viscoelastic properties of rubber nanocomposites filled with silica nanoparticles: A molecular dynamics simulation study. Chem Eng Sci. 2023;267:118318.
(21) Ou Z, Gao F, Zhao H, Dang S, Zhu L. Research on the thermal conductivity and dielectric properties of AlN and BN co-filled addition-cure liquid silicone rubber composites. RSC Adv. 2019;9(49):28851–6.
(22) Sun J, Wang D, Yao Y, Zeng X, Pan G, Huang Y, et al. Boron nitride microsphere/epoxy composites with enhanced thermal conductivity. High Volt. 2017;2(3):147–53.
(23) Li Y, Liu W, Shen F, Zhang G, Gong L, Zhao L, et al. Processing, thermal conductivity and flame retardant properties of silicone rubber filled with different geometries of thermally conductive fillers: A comparative study. Compos Part B-Eng. 2022;238:109907.
(24) Gao Z, Zhao L. Effect of nano-fillers on the thermal conductivity of epoxy composites with micro-Al2O3 particles. Mater Des (1980-2015). 2015;66:176–82.

(25) Guo G, Zhang J, Chen X, Zhao X, Deng J, Zhang G. Molecular-dynamics study on the thermodynamic properties of nano-SiO2 particle-doped silicone rubber composites. Comput Mater Sci. 2022;212:11571.
(26) Yang G, Qi X, Gao Q, Wang D. Electrical properties of nanosilica/epoxy resin modified by cooperation of plasma fluorination and coupling agent. High Volt Eng. 2022;48(2):689–97.
(27) Ding C, Liu L, Feng L. Effect of doped nano-SiO2, Al2O3, and polyhedral oligomeric sesquisiloxane on the thermodynamic properties of cellulose. AIP Adv. 2023;13:015104.
(28) Kim H, Jung D, Jung I, Cifuentes J, Rhee K, Hui D. Enhancement of mechanical properties of aluminium/epoxy composites with silane functionalization of aluminium powder. Compos Part B: Eng. 2012;43(4):1743–8.